Analyzing the Higher Order Structure of Proteins with Conformer-Selective Ultraviolet Photodissociation

Stephan Warnke,[†] Gert von Helden,[*,†] and Kevin Pagel[*,†,‡]

Fritz-Haber-Institut der Max-Planck-Gesellschaft, Faradayweg 4-6, 14195 Berlin, Germany

E-mail: helden@fhi-berlin.mpg.de; kevin.pagel@fu-berlin.de

Supporting Information

[*]To whom correspondence should be addressed

[†]Fritz Haber Institute of the Max Planck Society

[‡]Department of Biology, Chemistry, and Pharmacy, Institute of Chemistry and Biochemistry, Freie Universität Berlin, Takustr. 3, 14195 Berlin, Germany

Signal to Noise ratio in UVPD experiments

In Figure **S1**, a UVPD fragment mass spectrum (black) is shown together with the mass spectrum of the undissociated precursor ion (grey), exemplarily for conformer #7 from the conformer distribution shown in Figure 2 in the main manuscript. Many, sometimes only partially resolved signals can be observed, most of which have intensities way above the base line and can clearly be distinguished from noise signals. The UVPD fragment spectra of the other eight conformers are of similar intensities and S/N ratios.

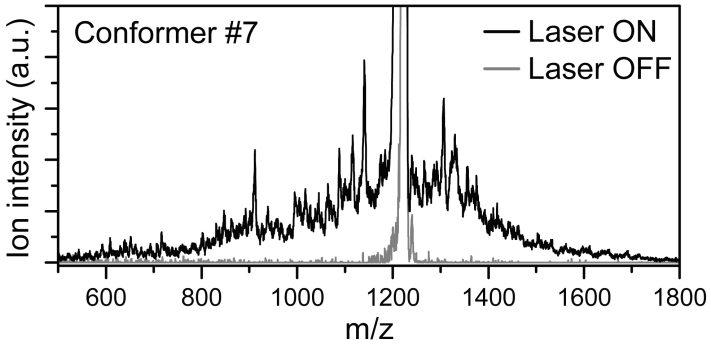

Figure S1: UVPD fragment mass spectrum (black) and mass spectrum of the undissociated precursor ion (grey) for comparison of the drift-time selected conformer #7.

Conformer-resolved collision induced dissociation

Experimental Setup

Sample preparation was carried out as described in the main manuscript.

Experiments were performed on a commercial Waters Synapt G2-S (Manchester, U.K.) MS/IMS/ToF-MS traveling-wave instrument.[1] For conformer-selective collision induced dissociation experiments (CID), the species of interest were m/z-selected by a quadrupole mass filter following conformer separation in an IMS cell. A high-pressure collision cell filled with argon was used to generate fragments, which were subsequently mass-analyzed by means of high-resolution ToF-MS.

Typical experimental settings were: source temperature, 20ąC; capillary voltage, 0.8-1.0 kV; sample cone, 40 V; source offset, 20 V; cone gas, off; trap collision energy, 2 V; trap gas flow, 2 mL/min; helium cell gas flow, 200 mL/min; IMS gas flow, 70 mL/min; trap DC bias, 34 V; IMS wave height, 40 V; IMS wave velocity, 650 m/s.

In traveling-wave instruments the effective ion temperature can increase substantially during injection and transmission through the IMS cell.[2,3] To observe compact or partially folded conformations of ubiquitin 7^+, the instrument therefore required careful tuning to gentle conditions, which was mainly achieved by reducing RF amplitudes, increasing the gas flow of the helium cell (which serves thermalization of the ions prior entering the high-pressure IMS region), and decreasing the IMS pressure and injection voltage (trap DC bias). For the acquisition of conformer-resolved CID spectra, the collision voltage in the argon-filled collision cell after conformer selection (i.e. the transfer cell) was raised until substantial fragmentation was observed (transfer CE 53.0 V - 54.5 V).

CID Fragment Spectra of ubiquitin 7^+ conformers

For comparison of fragmentation patterns and to test wether a conformational dependency can be found in CID, we analyzed the CID fragmentation behavior of the different 7^+ conformers shown in Figure 2 in the main manuscript. To do so, conformer-selective (low energy) CID experiments of ubiquitin 7^+ ions were performed on a commercially available Synapt G2-S MS/IM/ToF-MS instrument. Here, CID fragments are generated after conformer separation of the m/z-selected species and fragment spectra are acquired with high resolution, allowing an unambiguous fragment assignment using, for example, a complete list of possible fragments.

A typical ATD of ubiquitin 7^+ as measured on the Synapt instrument is shown in Figure **S2**. The distribution and relative abundances of the partially folded and extended structures are virtually identical to those observed at the DT instrument (Figure 2 in the main manuscript). Indicated in grey and consecutively labeled 1 to 9, are the drift-time windows

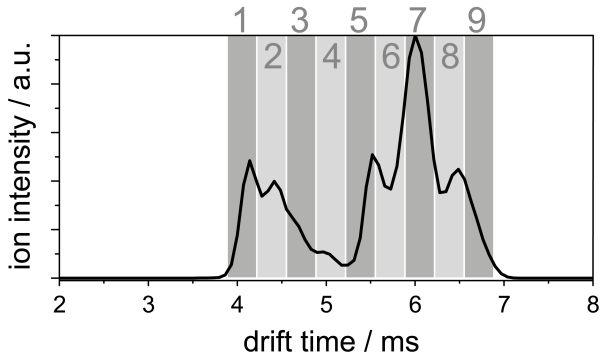

Figure S2: Arrival time distribution of ubiquitin 7^+, measured on the Synapt G2-S instrument. The conformer distribution observed here and on the drift tube instrument (Figure 2 in the main manuscript) are virtually identical. The grey bars labeled 1 to 9 consecutively indicate the regions of the ATD that were selected for extraction of CID fragment spectra.

for which fragment spectra were extracted. Each of these drift-time windows was selected such that they can be directly compared to the UVPD fragment spectra of the nine different ATD slices in Figure 2 in the main manuscript. The resulting CID fragment spectra corresponding to drift-time windows 1 to 9 in Figure **S2** are shown in Figure **S3**. The lower and higher m/z ranges are magnified by a factor of 40 and 5, respectively. The dashed lines indicate the positions of the assigned fragment types, which are annotated at the top of the figure and summarized in Table **S1**.

As reported previously, low energy CID of ubiquitin ions mainly yields b and y type fragments with a strong tendency for cleavages at the N-terminal side of the protein sequence.[4] A similar trend is also observed in this experiment and leads to a prominent series of C-terminal y-type fragments (starting at m/z 1306), which stem from cleavages of the peptide bonds between Glu^{18}-Pro^{19} (y_{58}^{5+}) and the five preceding residues Val^{17}-Glu^{18} (y_{59}^{5+}), Glu_{16}-Val_{17} (y_{60}^{5+}), Leu^{15}-Glu^{16} (y_{61}^{5+}), Thr^{14}-Leu^{15} (y_{62}^{5+}), and Ile^{13}-Thr^{14} (y_{63}^{5+}) with decreasing signal intensity towards the N-terminus. A second series of peaks stems from the same fragments at a higher charge state (6^+), but their intensity is considerably reduced corresponding to only a few percent of the lower-charged equivalents. Unlike in the UVPD experiments, however, no significant differences between the CID fragment spectra of the nine ubiquitin 7^+ conformers are observed. This is in good agreement with previous investigations, which showed that CID

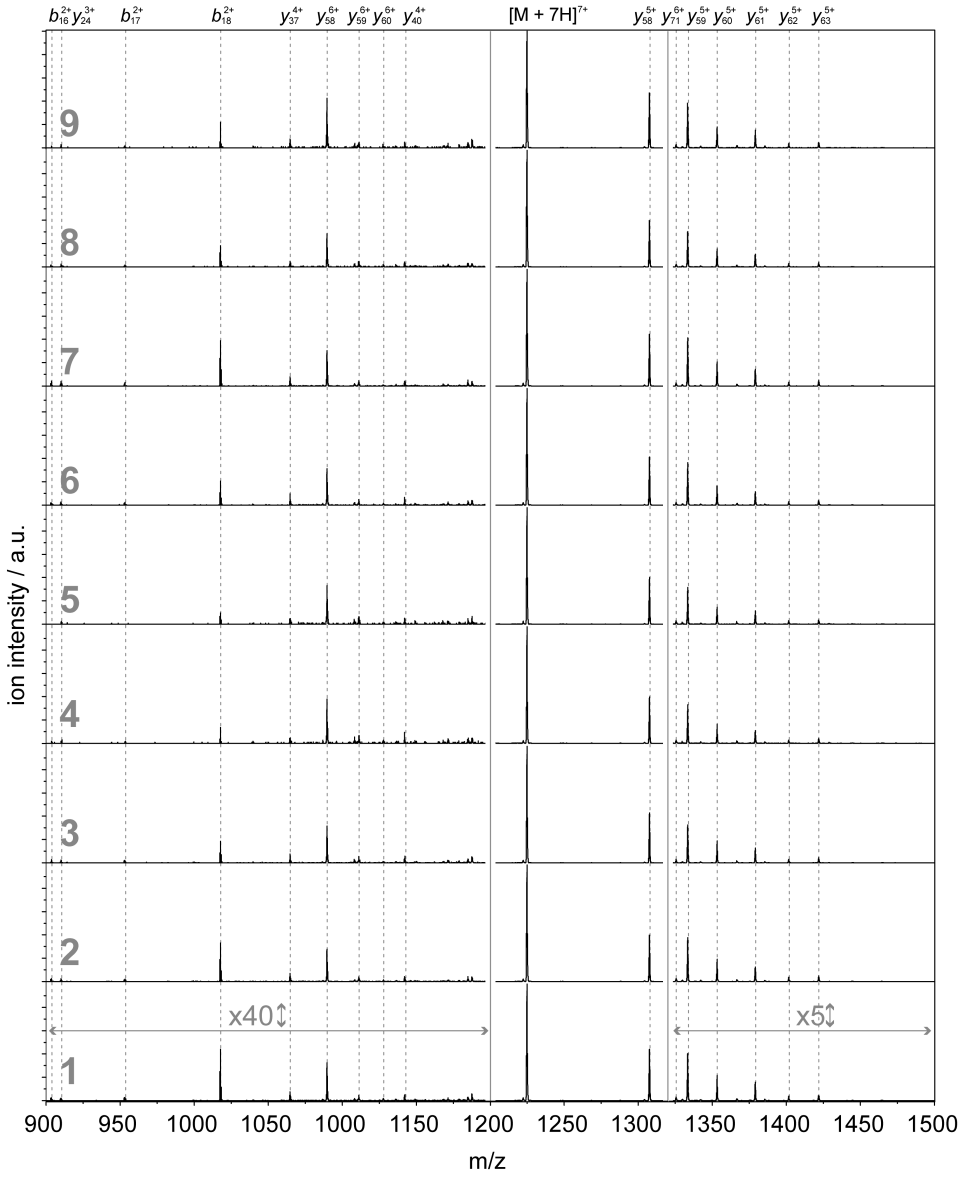

Figure S3: CID fragment spectra of the selected regions labeled 1 to 9 in the arrival time distribution (ATD) in Figure reffig:ATD. The spectra are normalized to the intensity of the precursor ion signal. The lower and higher m/z ranges are magnified by a factor of 40 and 5, respectively. The variation in intensity of the fragment at m/z 1020 (b_{18}^{2+}) lies within 0.5% and 2.5% of the strongest fragments and is therefore not considered significant.

is not sensitive to the higher order structure of proteins.[5,6] It is noteworthy, that a variation in abundance of a low intensity m/z 1017 fragment signal (b_{18}^{2+}) can be observed. However, the absolute intensity of this b_{18}^{2+} fragment, which is the N-terminal counterpart of the most intense y_{58}^{5+} fragment, only varies between 0.5% and 2% of the y_{58} signal and furthermore follows the relative intensity distribution of the precursor ion signal (compare relative intensities in Figure **S2**). It is likely that the intensity variation of this low abundance signal is an artifact of the measurement and is therefore considered to be not significant.

Comparison of fragments from different methods

CID and UVPD fragments

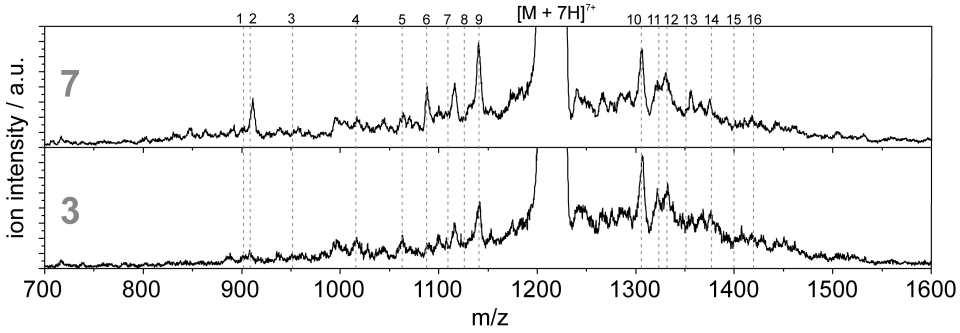

Figure S4: UVPD fragment spectra of the conformers #3 and #7 from Figure 3 in the main manuscript, as examples for group-A and group-B type conformers, and the positions of the most prominent CID fragments from Figure **S3** for comparison. The fragment types are listed in Table **S1**

In Figure **S4**, the positions of the 16 most prominent CID fragments from Figure **S3** are indicated as dashed lines (labeled **1-16**) in the UVPD fragment spectra of group-A and group-B conformers #3 and #7, respectively. A list of these fragments is given in Table **S1**. The fragments labeled **6**, **9**, **10**, **11**, and **12** are among the list of possible fragment candidates for the UVPD signals **II**, **IV**, **V**,**VI**, and **VII** in Figure 3 in the main manuscript. Most of these five y-type fragments stem from cleavage of Xxx-Pro peptide bonds, and have

been observed as UVPD fragments for ubiquitin 10^+ and 11^+.[7,8]

Table S1: List of the most prominent CID fragments, labeled in order of appearance from **1** to **16** for comparison with UVPD data (see Figure **S4**).

Label	*m/z*	Type	Sequence position
1	903.6	b_{16}	16
2	910.0	y_{24}	53
3	853.2	b_{17}	17
4	1017.7	b_{18}	18
5	1064.7	y_{37}	40
6	1089.6	y_{58}	19
7	1111.1	y_{59}	18
8	1127.6	y_{60}	17
9	1142.1	y_{40}	37
10	1307.3	y_{58}	19
11	1325.3	y_{71}	6
12	1333.1	y_{59}	18
13	1352.9	y_{60}	17
14	1378.8	y_{61}	16
15	1401.4	y_{62}	15
16	1421.6	y_{63}	14

ECD and UVPD fragments

In Figure **S5**, the UVPD fragment spectra of group-A and group-B conformers #3 and #7 are displayed together with observed fragments from electron capture dissociation (ECD) of ubiquitin 7^+ (dashed lines).[9] In the displayed *m/z* range, a few lower charged fragments are observed and only two fragments coincide with UVPD fragment signals (peaks **I** and **III** in Figure 3 in the main manuscript). However, none of these *c*-type fragments was earlier observed as UVPD fragments of ubiquitin (compare Table 1 in the main manuscript).

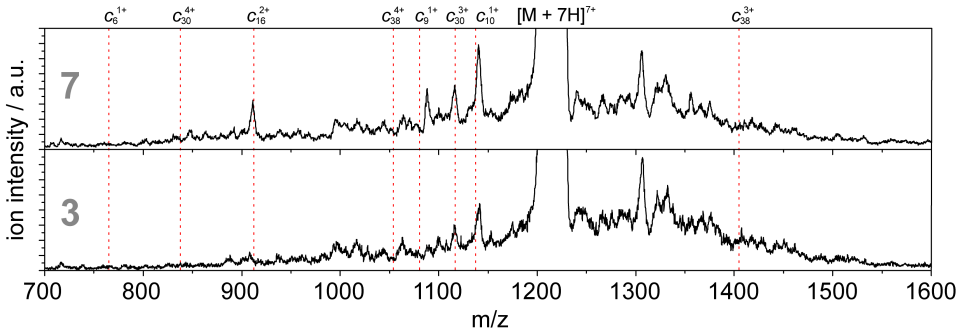

Figure S5: UVPD fragment spectra of group-A and group-B conformers #3 and #7 of ubiquitin 7^+, respectively, and fragments observed in electron capture dissociation (ECD) experiments of ubiquitin 7^+ (dashed lines) for comparison.[9]

References

(1) Pringle, S. D.; Giles, K.; Wildgoose, J. L.; Williams, J. P.; Slade, S. E.; Thalassinos, K.; Bateman, R. H.; Bowers, M. T.; Scrivens, J. H. *International Journal of Mass Spectrometry* **2007**, *261*, 1–12.

(2) Morsa, D.; Gabelica, V.; De Pauw, E. *Analytical Chemistry* **2011**, *83*, 5775–5782.

(3) Merenbloom, S. I.; Flick, T. G.; Williams, E. R. *Journal of the American Society for Mass Spectrometry* **2012**, *23*, 553–562.

(4) Reid, G.; Wu, J.; Chrisman, P.; Wells, J.; McLuckey, S. *Analytical Chemistry* **2001**, *73*, 3274–3281.

(5) Warnke, S.; Baldauf, C.; Bowers, M. T.; Pagel, K.; von Helden, G. *Journal of the American Chemical Society* **2014**, *136*, 10308–10314.

(6) Badman, E.; Hoaglund-Hyzer, C.; Clemmer, D. *Journal of the American Society for Mass Spectrometry* **2002**, *13*, 719–723.

(7) Shaw, J. B.; Li, W.; Holden, D. D.; Zhang, Y.; Griep-Raming, J.; Fellers, R. T.; Early, B. P.; Thomas, P. M.; Kelleher, N. L.; Brodbelt, J. S. *Journal of the American Chemical Society* **2013**, *135*, 12646–12651.

(8) Brodbelt, J. S. Unpublished UVPD fragment spectra of ubiquitin 10+ and 11+.

(9) Breuker, K.; Oh, H.; Horn, D. M.; Cerda, B. A.; McLafferty, F. W. *Journal of the American Chemical Society* **2002**, *124*, 6407–6420.